Spectrochimica Acta Part A: Molecular and Biomolecular Spectroscopy 133 (2014) 501–508

Contents lists available at ScienceDirect

Spectrochimica Acta Part A: Molecular and Biomolecular Spectroscopy

journal homepage: www.elsevier.com/locate/saa

Synthesis, photophysical and charge-transporting properties of a novel asymmetric indolo [3,2-b]carbazole derivative containing benzothiazole and diphenylamino moieties

Heping Shi [a,*], Jiandong Yuan [a], Xiuqing Dong [b], Fangqin Cheng [b,*]

[a] School of Chemistry and Chemical Engineering, Shanxi University, Taiyuan 030006, PR China
[b] State Environmental Protection Key Laboratory of Efficient Utilization Technology of Coal Waste Resources, Shanxi University, 92 Wucheng Road, Taiyuan 030006, Shanxi Province, PR China

HIGHLIGHTS

- A novel asymmetric indolo[3,2-b]carbazole compound was synthesized.
- The compound contains benzothiazole and diphenylamino moieties.
- The compound has strong intramolecular charge transfer character.
- The compound can be served as an excellent hole-transporting material in OLEDs.

GRAPHICAL ABSTRACT

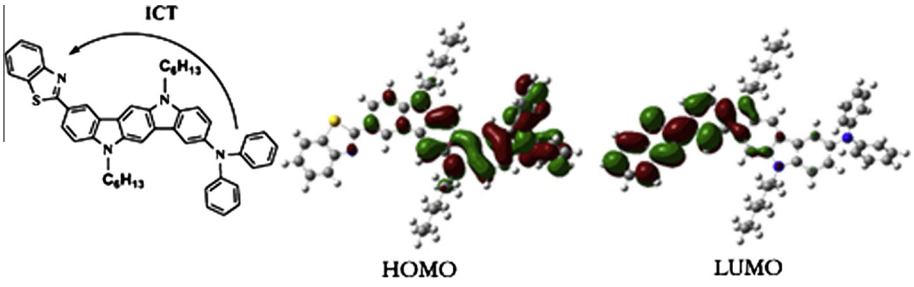

ARTICLE INFO

Article history:
Received 22 March 2014
Received in revised form 23 May 2014
Accepted 3 June 2014
Available online 13 June 2014

Keywords:
Synthesis
Indolo[3,2-b]carbazole
Benzothiazole
Diphenylamino
Photophysical properties
Charge-transporting properties

ABSTRACT

A novel asymmetric donor–π-donor–π-acceptor compound, 2-benzothiazolyl-8-diphenylamino-5,11-dihexylindolo[3,2-b]carbazole **(BDDAICZ)**, has been successfully synthesized by introducing a benzothiazole moiety (as an electron-acceptor) and a diphenylamino moiety (as an electron-donor) to 2-position and 8-position of indolo[3,2-b]carbazole moiety (as a skeleton and an electron-donor), and characterized by elemental analysis, ^{1}H NMR, ^{13}C NMR and MS. The thermal, electrochemical properties of **BDDAICZ** were characterized by thermogravimetric analysis combined with electrochemistry. The absorption and emission spectra of **BDDAICZ** was experimentally determined in several solvents and computed using density functional theory (DFT) and time-dependent density functional theory (TDDFT). The calculated absorption and emission wavelengths are coincident with the measured data. The ionization potential (IP), the electron affinity (EA) and reorganization energy of **BDDAICZ** were also investigated using density functional theory (DFT). Charge-transporting properties of **BDDAICZ** were characterized by OLEDs devices fabricated by using it as charge-transport layers. The results show that **BDDAICZ** has excellent thermal stability, electrochemical stability and hole-transporting properties, indicating its potential application as a hole-transporting material in OLEDs devices.

Introduction

Indolo[3,2-b]carbazole (ICZ) with a nitrogen atom as an electron donor is a promising heterocyclic compound. It can be easily functionalized by covalently linked to various groups to achieve different ICZ derivatives. The ICZ derivatives have the large planar

* Corresponding authors. Tel.: +86 351 7010588; fax: +86 351 7011688 (H. Shi). Tel./fax: +86 351 7018813 (F. Cheng).
E-mail addresses: hepingshi@sxu.edu.cn (H. Shi), cfangqin@sxu.edu.cn (F. Cheng).

http://dx.doi.org/10.1016/j.saa.2014.06.011
1386-1425/

and rigid conjugated structures together with remarkable photophysical properties, so these compounds have received much attention. Many ICZ derivatives with outstanding properties such as better morphological stability and thermal durability as well as desirable charge-injecting and transporting properties have been reported during the past decades. Ong and his co-workers reported a series of ICZ derivatives, which could be served as excellent hole-transporting materials and organic thin-film transistor (OTFT) materials [1–4]. Tao et al. designed and synthesized several ICZ derivatives, which can be used as excellent luminescence and hole-transporting materials in the OLEDs [5–7]. Boudreault et al. synthesized some new materials based on the ICZ framework, which were particularly suitable for OFET [8,9]. Grazulevicius and his co-workers developed various *N*,*N*-diarylated ICZ and these compounds can be served as hole-transporting materials for light emitting diodes [10–14]. Recently, Chen et al. reported two new ICZ derivatives with multi-functionality, which were employed as deep-blue emitters, hole-transporting materials and hosts to fabricate organic light-emitting devices (OLEDs) [15].

At present, the studies on synthesis and application of asymmetric indolo[3,2-b]carbazole derivatives are relatively limited [16,17]. Therefore, further studies are still necessary. In the present article, we report on the synthesis, structures and properties of a novel asymmetric indolo[3,2-b]carbazole derivative bearing a benzothiazole moiety as an electron-acceptor and a diphenylamino moiety as an electron-donor. The combination of indolo[3,2-b]carbazole with benzothiazole and diphenylamino was expected to obtain new charge-transporting materials with excellent performance. To the best of our knowledge, the study on this compound has never been reported. The synthetic details are illustrated in Scheme 1. The structure of the compound was characterized by elemental analysis, ^{1}H NMR, ^{13}C NMR and MS. Its photophysical properties were studied by UV–vis and fluorescence spectra, electrochemical properties were studied by cyclic voltammetry analysis, thermal property was studied by thermogravimetric analysis and charge-transporting properties were characterized by OLEDs devices fabricated by using it as charge-transport layers. In addition, its geometry, molecular orbitals, electronic absorption and emission spectra, charge-injection and transport properties were determined by quantum chemical calculations.

Experimental section

Synthesis of ***BDDAICZ***

All the reagents were purchased from commercial sources without further purification. All the reactions were carried out using Schlenk techniques under a nitrogen atmosphere. The synthesis of compound was described in Scheme 1. Cyclohexane-1, 4-dione-bis(p-bromophenyl)-hydrazone (compound **1**), 2,8-dibromoindolo[3,2-b]carbazole (compound **2**) and 2,8-dibromo-5, 11-dihexylindolo[3,2-b]carbazole (compound **3**) were synthesized according the literature procedures [18].

*Synthesis of cyclohexane-1,4-dione-bis (p-bromophenyl)-hy-drazone (compound **1**)*

1,4-Cyclohexanedione (5.62 g, 50 mmol) was dissolved in absolute ethanol (EtOH) (100 mL) and was added with stirring to a mixture of powdered 4-bromophenylhydrazine hydrochloride (22.4 g, 100 mmol), sodium acetate (8.2 g, 100 mmol) and absolute ethanol (200 mL) at room temperature. The mixture was quickly heated to 50 °C and kept stirring for 2 h, and then, the mixture was cooled to room temperature and poured into ice water with stirring. A precipitate was filtered off and washed carefully with water to give **1** yield 66%.

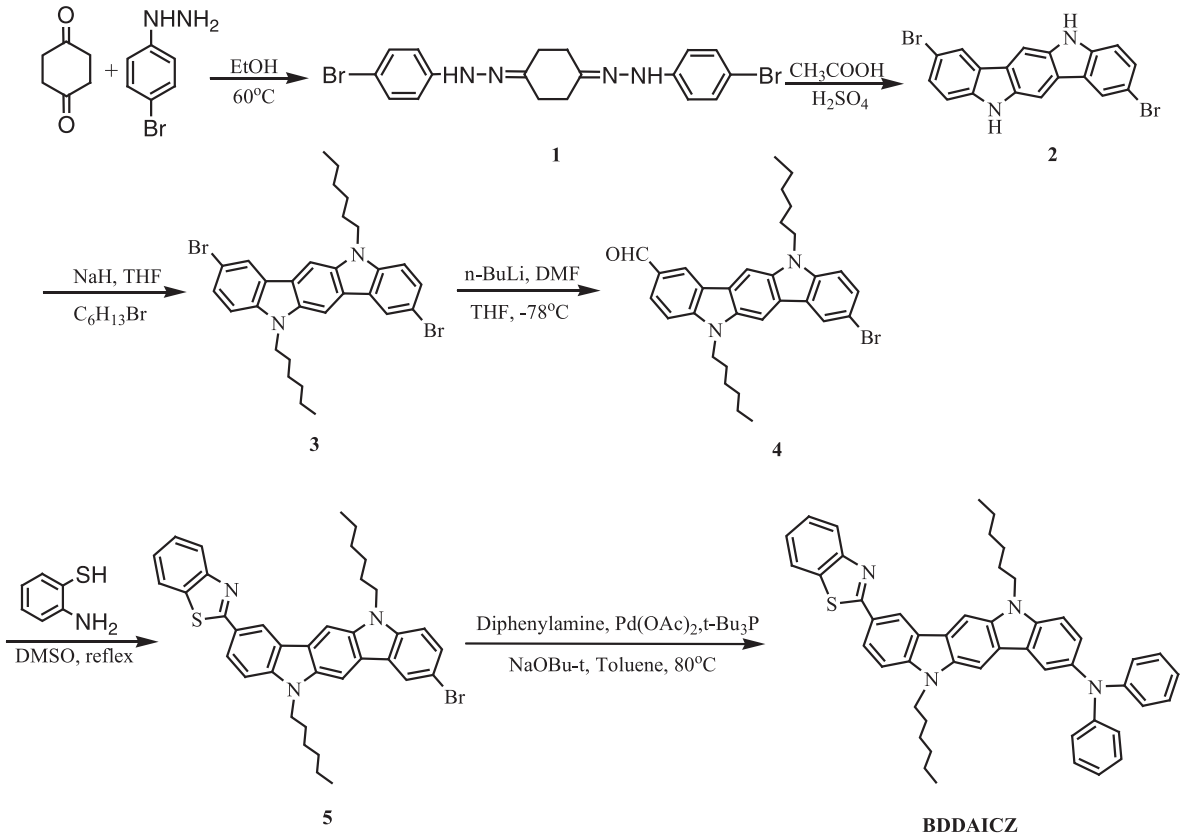

Scheme 1. The synthetic route of **BDDAICZ**.

*The synthesis of 2,8-dibromoindolo[3,2-b]carbazole (compound **2**)*

Compound **1** (10 g, 22 mmol) was added into a mixture of AcOH (130 mL) and H_2SO_4 (32 mL) at 0 °C and stirred for 5 min. The mixture was heated up to 30 °C and kept stirring for 1 h. Afterward, the mixture was further risen up to 60–70 °C and stirred for another 1 h. Then it was cooled down to room temperature and poured into ice water with stirring. The greenish solid was filtered off and washed with water and EtOH to neutral pH. Finally, dried and pure 2,8-dibromoindolo[3,2-b]carbazole (compound **2**) (4.88 g, yield 53.5%) was achieved. Mp > 300 °C. ^{1}H NMR (DMSO−d_6) δ 11.14 (2H, s, and N–H), and 7.1–8.24 (8H, m, and Ar–H).

*2,8-Dibromo-5,11-dihexyl-indolo[3,2-b]carbazole (compound **3**)*

To a solution of 2, 8-dibromoindolo[3,2-b]carbazole (2 g, 4.8 mmol) in anhydrous THF (50 mL) in the round-bottomed flask, NaH 0.35 g (14.4 mmol) was added under a nitrogen atmosphere and the solution was cooled to 0 °C, then the reaction mixture was heated to 55 °C for 6 h. The reaction mixture was cooled to 0 °C again, and 1-bromohexane (1.96 mL, 14 mmol) was added to the reaction mixture slowly. The mixture was heated to 65 °C for 36 h, and then poured into water (250 mL) and the precipitate was afforded. The precipitate was filtered and washed with ethanol (100 mL). And the pure product was obtained by column chromatography as a yellow solid (2.56 g, 91.5%). M.p.: 232.6–233.2 °C. ^{1}H NMR (600 MHz, $CDCl_3$) δ 8.30 (d, *J* = 1.8 Hz, 2H), 7.93 (s, 2H), 7.55 (dd, *J* = 1.8, 1.8 Hz, 2H), 7.26 (d, *J* = 7.2 Hz, 2H), 4.34 (t, *J* = 7.2 Hz, 4H), 1.91 (t, *J* = 7.2 Hz, 4H), 1.43 (s, 4H), 1.33–1.29 (m, 8H), 0.87 (t, *J* = 7.1 Hz, 6H).

*8-bromo-5,11-dihexyl-indolo[3,2-b]carbazole-2-carbaldehyde (compound **4**)*

Compound **3** (0.6 g, 1.03 mmol) was dissolved in anhydrous THF (50 mL) under a nitrogen atmosphere. The solution was cooled to −78 °C, and n-butyllithium (0.329 mL, 0.8 mmol) was added into it dropwise. The reaction mixture was stirred for 1 h at −78 °C, and the temperature of the reaction mixture was raised to −50 °C. After being stirred for 0.5 h, the reaction mixture was cooled to −78 °C again. A solution of DMF (1 mL, 12.9 mmol) was added into dropwise at the temperature. Then the reaction mixture was stirred for another 1 h. The reaction solution was allowed to be warmed to room temperature and diluted with CH_2Cl_2. The organic layer was washed with water, dried over $MgSO_4$ and filtered and evaporated under vacuum. The residue was purified by column chromatography to afford 8-bromo-5, 11-dihexyl-indolo[3,2-b]carbazole-2-carbaldehyde **4** as a yellow solid (0.39 g, 71.3%). M.p.: 230–231.5 °C. ^{1}H NMR (600 MHz, $CDCl_3$) δ 10.11 (s, 1H), 8.72 (d, *J* = 0.9 Hz, 1H), 8.31 (d, *J* = 1.7 Hz, 1H), 8.06 (s, 1H), 8.01 (dd, *J* = 8.4, 1.3 Hz, 1H), 7.98 (s, 1H), 7.57 (dd, *J* = 8.6, 1.8 Hz, 1H), 7.46 (d, *J* = 8.5 Hz, 1H), 7.30 (d, *J* = 8.6 Hz, 1H), 4.39 (dt, *J* = 22.3, 7.3 Hz, 4H), 1.99–1.90 (m, 4H), 1.48–1.41 (m, 4H), 1.38–1.29 (m, 8H), 0.88 (td, *J* = 7.1, 2.9 Hz, 6H). ^{13}C NMR (151 MHz, $CDCl_3$) δ 191.54, 145.24, 141.90, 141.84, 136.73, 136.37, 128.45, 127.80, 126.14, 123.58, 123.28, 122.98, 122.66, 122.62, 120.31, 118.26, 108.59, 108.40, 99.57, 99.27, 43.64, 43.45, 31.65, 31.56, 28.82, 28.76, 27.09, 26.99, 22.56, 22.52, 13.98, 13.95. MS (*m*/*z*): 530.15 (M+). Anal. Calcd. for $C_{31}H_{35}BrN_2O$: C, 70.05%; H, 6.64%; N, 5.27%; Found: C, 69.81%; H, 6.57%; N, 5.22%.

*8-(Benzothiazol-2-yl)-2-bromo-5,11-dihexyl-indolo[3,2-b]carbazole (compound **5**)*

The mixture of **4** (0.531 g, 1 mmol), 2-aminothiophenol (0.16 mL, 1.5 mmol) and DMSO (50 mL) was heated to 180 °C in an oil bath, and held at the temperature for 12 h. Subsequently, the reaction mixture was cooled to room temperature, then poured into water and extracted with CH_2Cl_2 (3 × 30 mL). The combined organic layer was dried over anhydrous $MgSO_4$ and evaporated to dryness. The crude compound was stirred for 15 min in ethanol (30 mL) and then filtered. The pure product was obtained by column chromatography as a yellow-green solid (0.53 g, yield: 83.2%). M.p.: 241.9–242.9 °C. ^{1}H NMR (600 MHz, $CDCl_3$) δ 9.03 (s, 1H), 8.32 (d, *J* = 1.8 Hz, 1H), 8.20 (dd, *J* = 8.5, 1.4 Hz, 1H), 8.13 (d, *J* = 7.6 Hz, 2H), 7.97 (s, 1H), 7.91 (d, *J* = 7.8 Hz, 1H), 7.56 (dd, *J* = 8.6, 1.8 Hz, 1H), 7.51 (t, *J* = 7.6 Hz, 1H), 7.46 (d, *J* = 8.5 Hz, 1H), 7.38 (t, *J* = 7.5 Hz, 1H), 7.30 (d, *J* = 8.6 Hz, 1H), 4.44–4.38 (m, 4H), 1.96 (qd, *J* = 15.0, 7.5 Hz, 4H), 1.46 (dd, *J* = 13.8, 7.3 Hz, 4H), 1.39–1.30 (m, 8H), 0.89 (td, *J* = 7.2, 2.1 Hz, 6H). Anal. Calcd. for $C_{37}H_{38}BrN_3S$: C, 69.80%; H, 6.02%; N, 6.60%; Found: C, 69.12%; H, 5.96%; N, 6.54%.

*2-benzothiazolyl-8-diphenylamino-5, 11-dihexylindolo[3,2-b]carbazole (**BDDAICZ**)*

Compound **5** (185 mg, 0.29 mmol) and diphenylamino (196 mg, 1.16 mmol) were mixed with dry toluene (50 ml) in a two necked round bottomed flash containing a stir bar. The $Pd(OAc)_2$ (10 mol%), t-Bu_3P (10 mol%), and NaOBu-t (111 mg, 1.16 mmol) were also added and the mixture was stirred under nitrogen at 80 °C for about 15 h. After cooling, the reaction was quenched by adding water and then was extracted with CH_2Cl_2. The organic layer was dried over anhydrous $MgSO_4$ and evaporated under vacuum. The product was purified by silica gel column chromatography using CH_2Cl_2/hexane (vol. ratio 1:2) as an eluant. Yield: 155 mg (74%) of yellow solid. M.p.: 220–222 °C. ^{1}H NMR (600 MHz, $CDCl_3$) δ 9.16 (s, 1H), 8.29 (dd, *J* = 17.0, 8.0 Hz, 2H), 8.24–8.13 (m, 1H), 8.00 (d, *J* = 17.9 Hz, 1H), 7.86 (d, *J* = 7.9 Hz, 2H), 7.54 (t, *J* = 7.6 Hz, 1H), 7.48–7.43 (m, 1H), 7.41 (t, *J* = 7.5 Hz, 2H), 7.33 (dd, *J* = 9.9, 7.6 Hz, 2H), 7.25–7.06 (m, 7H), 6.96 (s, 2H), 4.49–4.29 (m, 4H), 2.01–1.89 (m, 4H), 1.55–1.49 (m, 2H), 1.43–1.29 (m, 10H), 0.90–0.84 (m, 6H). ^{13}C NMR (151 MHz, $CDCl_3$) δ 173.69, 151.71, 147.04, 142.13, 141.86, 139.21, 138.12, 137.32, 131.95, 130.12, 129.13, 128.40, 126.60, 126.44, 126.17, 125.54, 124.34, 123.91, 121.91, 112.42, 111.85, 46.58, 34.58, 34.45, 32.57, 32.53, 30.02, 29.86, 25.50, 25.40, 16.92, 16.83. MS (*m*/*z*): 724.36 (M+). Anal. Calcd. for $C_{49}H_{48}N_4S$: C, 81.18%; H, 6.67%; N, 7.73%; Found: C, 80.96%; H, 6.6%; N, 7.65%.

Measurement and characterization

Melting points were determined with a WRS-1B melting point detector. All the NMR spectra were measured with a Bruker Avance 600 MHz NMR spectrometer. Thermogravimetric analyses were performed with a TA TGA 2050 thermogravimetric analyzer under nitrogen atmosphere with a heating rate of 20 °C/min from room temperature to 600 °C. Elemental analyses were performed with an Elementar Analysensysteme (GmbH). Mass spectra were recorded with the LC–MS system consisted of a Waters 1525 pump and a Micromass ZQ4000 singlequadrupole mass spectrometer detector (Waters). Cyclic voltammetry experiments were carried out with a CHI-600C electrochemical analyzer. The measurements were performed with a conventional three-electrode configuration consisting of a glassy carbon working electrode, a platinum-disk auxiliary electrode and an Ag/AgCl reference electrode. The scan speed of the measurements is 50 mV/s. UV–vis absorption spectra were obtained from a Shimadzu UV-2450 spectrophotometer. Fluorescence spectra were taken from a Shimadzu RF-5301PC fluorescence spectrometer. All the spectral experiments were carried out at room temperature.

Device fabrication and measurement

The multilayer OLEDs were fabricated by the vacuum-deposition method. Organic layers were deposited by high-vacuum (5×10^{-4} Pa) thermal evaporation onto a glass (3 cm × 4 cm)

substrate pre-coated with an indium tin oxide (ITO) layer. The ITO surface was cleaned ultrasonically sequentially with acetone, methanol, and deionized water and then it was treated with UV-ozone. All organic layers were sequentially deposited. Thermal deposition rates for organic materials, LiF and Al were 0.5, 0.5 and 1 Å s^{-1}, respectively. The active area of the devices was 12 mm^2. The current-characteristics of the OLEDs devices were measured with Keithley 2400 Source Meter. All measurements were done at room temperature under ambient conditions.

Theoretical calculation

The neutral and ionic geometries of **BDDAICZ** in ground-state were optimized by density functional theory (DFT) method at B3LYP level with 6-31G (d, p) basis set [19,20]. The frontier molecular orbital characteristics were analyzed on the optimized structures at the same level. The ionization potential (IP), electron affinity (EA), reorganization energy and HOMO–LUMO gap of **BDDAICZ** were also calculated by DFT method based on the optimized geometry of the neutral and ionic molecules. The excited-state geometry of **BDDAICZ** was optimized using time-dependent density functional theory (TDDFT) method at B3LYP level with 6-31G (d, p) basis set [21]. The absorption spectra and the emission spectra of this compound were carried out using TDDFT method based on the optimized ground state structures and the lowest singlet excited-state structures, respectively. Solvent effects were also taken into account in these calculations by using the polarized continuum model (PCM) [22,23]. All calculations were carried out with the Gaussian09 program package using the advanced computing facilities of supercomputing center of computer network information center of Chinese Academy of Sciences [24].

Results and discussion

*Synthesis and thermal properties of **BDDAICZ***

Scheme 1 Outlines the synthesis of **BDDAICZ**. Firstly, compound **1** was prepared via the reaction of 1,4-Cyclohexanedione with 4-bromophenylhydrazine, then compound **2** was synthesized by the Fischer reaction of compound **1** in a mixture of acetic acid and H_2SO_4 at 65 °C in high yield. Secondly, compound **3** was obtained via the reaction of indolo[3,2-b]carbazole, NaH and 1-bromohexane in 91.5% yield. Thirdly, compound **4** was obtained as the key intermediate for the whole procedure via the bromine–lithium exchange reactions of compound **3** with n-BuLi and reacting with DMF under nitrogen atmosphere in 71.3% yield. After that, compound **5** was prepared in 83.2% yield by the condensation reaction of compound **4** with 2-aminothiophenol in DMSO at 180 °C. Finally, the compound **BDDAICZ** was synthesized via the Buchwald–Hartwig coupling reaction of compound **5** with diphenylamino under nitrogen in the presence of $Pd(OAC)_2$, t-Bu3P and NaOBu-t as a catalytic system in 74% yield. Structure of **BDDAICZ** was confirmed by NMR, MS and elemental analysis. Further details are given in the experimental section. **BDDAICZ** is soluble in many of the common organic solvents such as dichloromethane, chloroform, dimethylformamide, tetrahydrofuran, toluene and dimethylsulfoxide. The thermal properties of **BDDAICZ** were investigated by thermogravimetric analysis (TGA) under a nitrogen atmosphere. The TGA curve of **BDDAICZ** is shown in Fig. S1. Fig. S1 is placed in electronic supplementary information (ESI). The TGA result of **BDDAICZ** show 5% weight loss temperature is higher than 193 °C, indicating that **BDDAICZ** has good thermal stability and should be adequate for most optoelectronic device applications.

*The molecular structure and frontier orbitals of **BDDAICZ***

The molecular structures of **BDDAICZ** in different polar solvents were optimized using DFT method at the DFT/B3LYP/6-31G (d, p) level with the polarized continuum model (PCM). The optimized geometry of **BDDAICZ** shows that the indolo[3,2-b]carbazole and benzothiazole moieties are of planar structure and the diphenylamino group forms propeller-like conformation originated from the trigonal nitrogen center as well as molecular structures have only slight differences in different polar solvents. The optimized structure in THF solvent is shown in Fig. 1. The values of the parameters are listed in Table 1.

The frontier molecular orbitals, three highest occupied molecular orbitals (HOMO−2, HOMO−1 and HOMO) and six lowest unoccupied molecular orbitals (LUMO, LUMO+1, LUMO+2, LUMO+3, LUMO+4, LUMO+5) of **BDDAICZ** were analyzed based on the optimized structures in different polar solvents. The diagrams of these orbitals in THF solvent are placed in Fig. 2. As shown in Fig. 2, The HOMO is localized mainly on diphenylamino moiety, the HOMO−1 is localized mainly on diphenylamino and indolo[3,2-b]carbazole moieties and the HOMO−2 is localized mainly on diphenylamino moiety, while the LUMO is localized mainly on benzothiazole moiety, the LUMO+1 is localized mainly on indolo[3,2-b]carbazole moiety and the LUMO+5 is localized mainly on diphenylamino moiety. Therefore, the electronic transition from the ground state to the first excited state mainly involves the intramolecular charge transfer (ICT) from the diphenylamino moiety (as electron-donor) and indolo[3,2-b]carbazole moiety (as electron-donor) to benzothiazole moiety (as electron-acceptor). Generally, holes and electrons in OLEDs are transferred through the individual HOMO and LUMO levels [25]. Fig. 2 shows that **BDDAICZ** exhibits almost complete separation of LUMO and HOMO. The almost complete localization of HOMO and LUMO means that the HOMO to LUMO transition becomes a typical charge transfer transition, this is essential for the efficient hole and electron transport [26]. The calculated HOMO energy level, LUMO energy level and HOMO–LUMO gap are −4.72 to −4.78 eV, −1.44 to −1.50 eV and 3.25–3.29 eV in different polar solvents. These data are collected in Table 2.

*Photophysical properties of **BDDAICZ***

*UV–vis spectra of **BDDAICZ***

UV–vis absorption spectra of **BDDAICZ** in various solvents of different polarity (1.0×10^{-5} M) are presented in Fig. 3. The

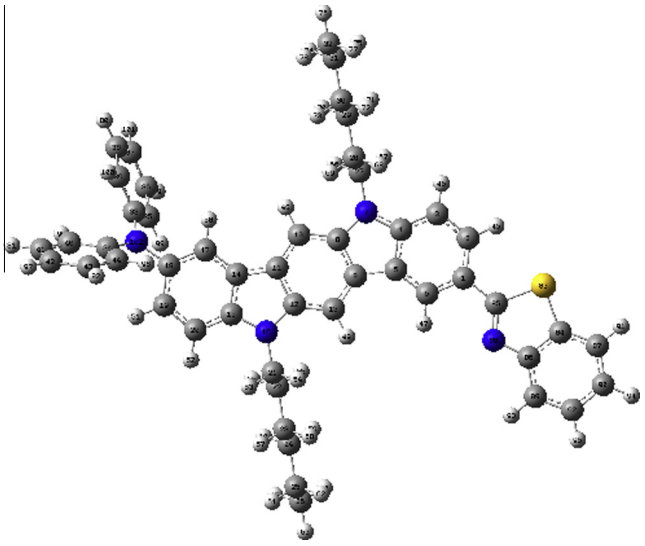

Fig. 1. The optimized geometry of **BDDAICZ** in THF solvent.

Table 1
Selected bond length and dihedral angle of the optimized structures of **BDDAICZ** in its ground state and excited state in THF solvent.

Parameters	The ground state	The excited state
Bond length (Å)		
C1–C85	1.46362	1.45878
C18–N102	1.43141	1.40480
C33–N102	1.41772	1.42125
C34–N102	1.41760	1.42219
C85–N88	1.30217	1.30635
C85–S83	1.79549	1.80384
Dihedral angle (°)		
C2–C1–C85–N88	179.72130	178.50773
C2–C1–C85–S83	−0.25640	−1.61660
C6–C1–C85–N88	−0.10353	−1.25204
C6–C1–C85–S83	179.91878	178.62363
C17–C18–N102–C33	53.77483	34.20806
C17–C18–N102–C34	−125.17283	−145.73058
C19–C18–N102–C33	−125.99306	−145.83987
C19–C18–N102–C34	55.05928	34.22149

UV–vis absorption spectra data are listed in Table 3. As depicted in Fig. 3, the absorption spectra of **BDDAICZ** show two similar absorption bands, a high-energy absorption band at 290–320 nm and a low-energy absorption band at 320–430 nm, in which the high-energy absorption band is attributed to π–π* transition of the indolo[3,2-b]carbazole backbone and the low-energy absorption band is attributed to π–π* transition of the intramolecular charge transfer (ICT) from the diphenylamino moiety (as an electron-donor) and indolo[3,2-b]carbazole (as an electron-donor) to benzothiazole moiety (as an electron-acceptor) [27].

In order to gain a detailed insight into the nature of the UV–vis absorption of **BDDAICZ** observed experimentally, we computed singlet–singlet electronic transition in different polar solvents based on the optimized geometries of the ground state of **BDDAICZ** using time-dependent DFT method at the B3LYP/6-31G (d, p) level with the polarized continuum model (PCM). The computed data are collected in Table S1 (ESI). On the basis of the calculated vertical excited energy and their corresponding oscillator strengths, the continuous electronic absorption spectrum was simulated with the help of SWIZARD software. The simulated electronic absorption spectrum of **BDDAICZ** is shown in Fig. S2 (ESI). As seen in Fig. S2 and Table S1, The absorption band at about 320–430 nm is derived from the π–π* transitions of intramolecular charge transfer (ICT) from the diphenylamino moiety (as an electron-donor) and indolo[3,2-b]carbazole moiety (as an electron-donor) to benzothiazole moiety (as an electron-acceptor) owing to the lower-energy electronic transition from HOMO to LUMO, HOMO to LUMO+1, HOMO−2 to LUMO and HOMO−2 to LUMO+1. The absorption bands at 290–320 nm are ascribed to the π–π* transitions of the conjugated molecular backbone owing to the higher-energy electronic transition from HOMO to LUMO+5. The calculated results are consistent well with the experimental results.

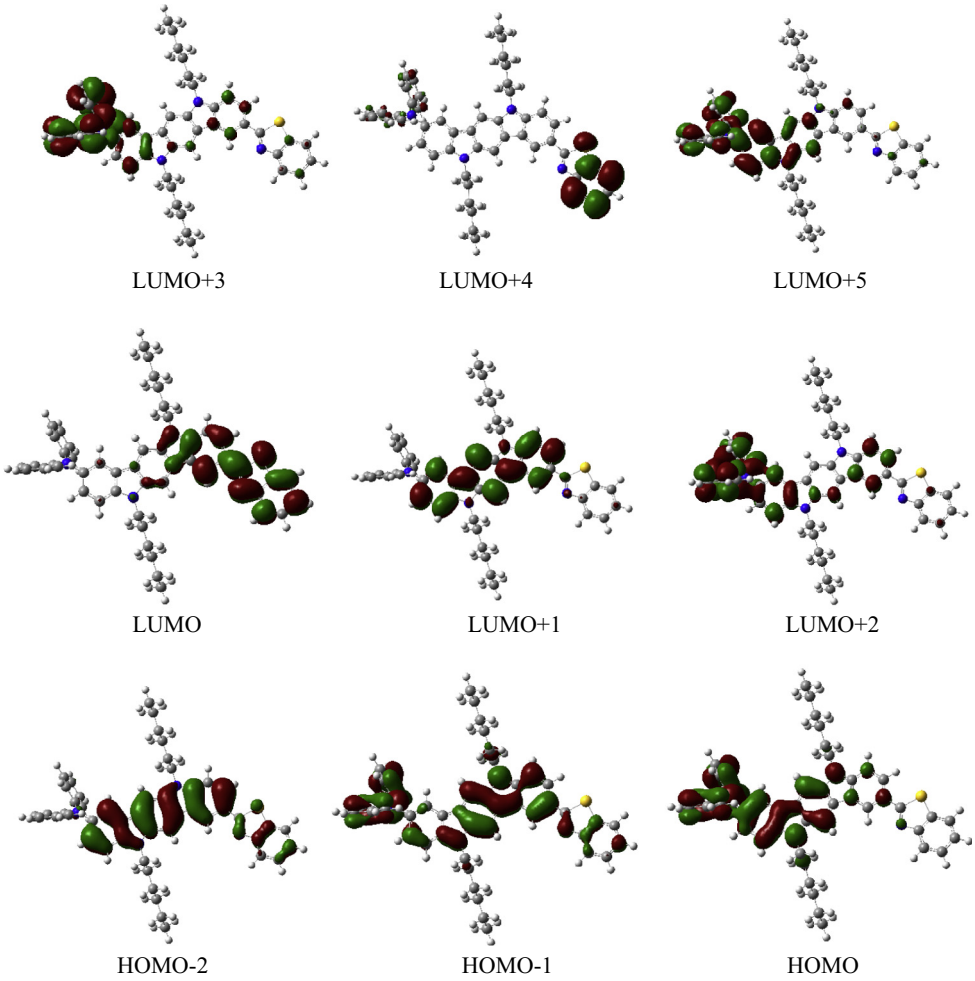

Fig. 2. The frontier molecular orbitals of **BDDAICZ** in the ground state in THF solvent.

Table 2
HOMO and LUMO energies level, and HOMO–LUMO gap of **BDDAICZ** obtained from DFT/B3LYP/6-31G (d, p) calculation in different solvents and experimental measurement in Acetonitrile.

Methods	Solvents	HOMO (eV)	LUMO (eV)	ΔE (eV)
Theoretical calculation	Hex	−4.72	−1.47	3.25
	Dichloromethane	−4.76	−1.49	3.27
	THF	−4.73	−1.44	3.29
	Acetonitrile	−4.78	−1.5	3.28
	DMSO	−4.78	−1.5	3.28
Experimental measurement	Acetonitrile	−5.02	−2.03	2.99

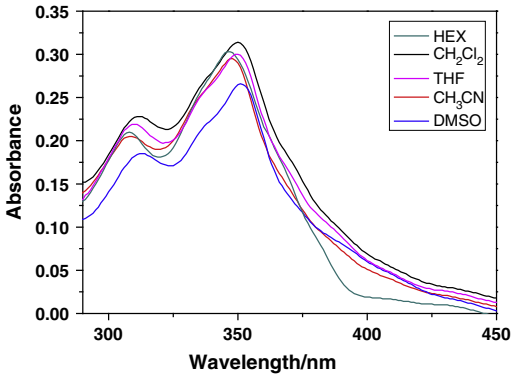

Fig. 3. UV–vis absorption spectra of **BDDAICZ** in different solvents.

*Fluorescence spectra of **BDDAICZ***

Fig. 4 shows the steady-state fluorescence spectra for **BDDAICZ** in several different polarity solvents (1.0×10^{-5} M). Fluorescence spectra data were listed in Table 3. As shown in Fig. 4 and Table 3, **BDDAICZ** possesses mainly a broad emission band in several solvents except in hexane, which is mainly originated from overlap of the π–π* transition of the conjugated molecular backbone and the intramolecular charge transfer (ICT) from the diphenylamino moiety to the benzothiazole moiety. In addition, **BDDAICZ** presents significant solvatochromism and a bathochromic shift of 45 nm ranging from 453 nm (in hexane) to 498 nm (in DMSO) with the increasing polarity of the solvents. Such a remarkably solvatochromism suggests that the intramolecular charge transfer (ICT) from the diphenylamino moiety to the benzothiazole moiety takes place in the excitation process and the polar solvents are propitious to the ICT process.

In order to gain insight into the nature of the fluorescence emission observed for **BDDAICZ**, we optimized its geometries of the excited states using TDDFT method at the B3LYP/6-31G (d, p) level with the polarized continuum model (PCM). The data of optimized structure in THF solvent are also listed in Table 1. Based on the optimized structures, we calculated their electronic transitions

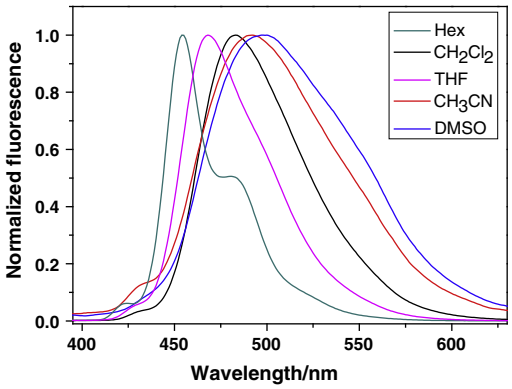

Fig. 4. Fluorescence spectra of **BDDAICZ** in different solvents. Excited at 350 nm.

energy from the excited states to the ground states. The computed data are collected in Table S2 (ESI). On the basis of the calculated vertical transitions energy and their corresponding oscillator strengths, the continuous electronic emission spectrum was simulated with the help of SWIZARD software. The simulated emission spectra of **BDDAICZ** are shown in Fig. S3 (ESI). As can be seen in Fig. S3, the simulated maximum emission wavelengths of **BDDAICZ** are around 439–516 nm in different polar solvents. The emission wavelengths are mainly originated from the intramolecular charge transfer (ICT) from the diphenylamino moiety (as an electron-donor) and indolo[3,2-b]carbazole (as an electron-donor) to benzothiazole moiety (as an electron-acceptor) owing to the π–π* transition from HOMO to LUMO and the molecular backbone owing to the π–π* transition from HOMO to LUMO+1. The simulated emission spectra are in relatively good agreement with the experimental fluorescence spectra.

According to the published work [28], solvatochromic shifts may be described by the state and excited dipole moments in different polar solvents. In order to gain insight into the nature of significant solvatochromism, we computed the state and excited dipole moments of **BDDAICZ** in different polar solvents. The data are listed Table 4. Table 4 show **BDDAICZ** has the large difference between the excited- and state-dipole moments. The large difference indicates the strong intramolecular charge transfer and significant solvatochromism. Our results are similar with those of the reported work [29–31].

*The fluorescence quantum yields and lifetimes of **BDDAICZ***

The fluorescence quantum yields (Φ) of **BDDAICZ** were measured in the several solvents using quinine bisulfate in 0.1 mol/L sulfuric acid as a standard, which were carried out at room temperature. The fluorescence quantum yield was calculated from Eq. (1) [32].

$$\phi_s = \phi_r \frac{F_s}{F_r} \frac{A_r}{A_s} \left(\frac{n_r}{n_s}\right)^2 \quad (1)$$

Table 3
Photophysical properties of **BDDAICZ** in several solvents.

Solvents	UV wavelength, λ (nm)	FL wavelength, λ (nm)	Stokes shift (cm^{-1})	Fluorescence quantum yields (Φ)	Fluorescence lifetime, τ (ns)
Hex	307, 346	454	10546, 6875	0.102	1.72, 4.91
Dichloromethane	311, 350	483	11450, 7867	0.016	1.52, 7.47
THF	309, 350	468	10994, 7203	0.084	1.16, 7.43
Acetonitrile	307, 347	492	12248, 8493	0.017	2.72, 7.51
DMSO	311, 351	499	12114, 8450	0.085	2.75, 7.63

where Φ is the fluorescence quantum yield, F is the integration of the emission intensities, A is the absorbance at the excitation wavelength, n is refractive index of the solution and the subscripts "r" and "s" denote reference and sample, respectively. The data are summarized in Table 3. The fluorescence decay behaviors of **BDDAICZ** were also studied in the several solvents. Typical fluorescence decay curve of **BDDAICZ** are displayed in Fig. S4 (ESI). It is easily found that the fluorescence decay curves in several solvents are multi-exponential model. The fluorescence lifetimes are also collected in Table 3.

*Electrochemical properties of **BDDAICZ***

The electrochemical properties of **BDDAICZ** were explored through cyclic voltammetry (CV) in 1.0×10^{-3} M MeCN solution. The CVs were performed using the Ag/AgCl as the reference electrode and 0.1 mol/L of tetrabutylammonium perchlorate in anhydrous MeCN as the supporting electrolyte under a nitrogen atmosphere. The CV curve is shown in Fig. S5 (ESI). Onset oxidation potential is observed at 0.62 V. Thus, the HOMO and LUMO energy levels was calculated by using the empirical formula HOMO = $-(E_{ox} + 4.40)$ from the onset of the first oxidation [33]. $E_{LUMO} = E_{HOMO} - E_g$, and the optical energy gaps were derived from the lowest energy absorption onset in the absorption spectra, which is 2.99 eV. The HOMO and LUMO energies and energy difference $E_{LUMO-HOMO}$ of **BDDAICZ** are listed in Table 2. As shown in Table 2, the calculated HOMO and LUMO levels in different polar solvents are higher than the experimental values. The calculated HOMO–LUMO gaps in different polar solvents slightly deviate from those obtained from the experimental results (ca. 0.26–0.30 eV). As we all know, the values of HOMO and LUMO usually determine the hole and electron injection of the materials which is in accord with the work function values of cathode and anode, and the hole-transporting material (HTM) with the smaller negative value of HOMO should lose their electrons more easily, while the electron-transporting material (ETM) with larger negative value of LUMO should accept electrons more easily. It can be seen from Table 2 that the HOMO level of **BDDAICZ** matches well with the work function of the indium tin oxides (ITOs) from −4.8 to −5.1 eV. This implies that **BDDAICZ** is promising as hole injection and transport materials in OLEDs [34].

*Charge-transporting properties of **BDDAICZ***

The charge injection and transport ability are important parameters for OLEDs. In general, the lower the ionization potential (IP), the easier the entrance of holes from ITO to hole-transport layer (HTL). The higher the electronic affinity (EA), the easier the entrance of electrons from cathode to electron-transport layer (ETL). And the charge transport rate can be approximated by the Marcus electron-transfer theory, which is mainly decided by hole/electron reorganization energy according to this theory [35,36]. In order to evaluate the charge-injection and transport properties, the ionization potential (IP), electronic affinity (EA) and hole/electron reorganization energy of **BDDAICZ** are calculated and collected in Table 5**.** As shown in Table 5, **BDDAICZ** has lower IP value [37,38] and a small hole reorganization energy compared with electron reorganization energy in different polar solvents, suggesting its potential application as the hole-transport material.

Table 4
Ground and excited state dipole moments of **BDDAICZ** computed in different polar solvents.

Solvents	Hex	Dichloromethane	THF	Acetonitrile	DMSO
Dipole moments (ground state)	0.9749	1.1328	1.1179	1.1855	1.1903
Dipole moments (excited state)	1.5224	2.1102	2.0595	3.2663	3.2815

Table 5
Ionization potential (IP), electron affinity (EA) and reorganization energy of **BDDAICZ** obtained from DFT/B3LYP/6-31G (d, p) calculation (eV) in different solvents.

Solvents	IP_v	IP_a	λ_{Hol}	EA_v	EA_a	λ_{Ele}
Hex	5.152	5.026	0.282	0.835	0.939	0.317
Dichloromethane	4.763	4.607	0.287	1.454	1.612	0.327
THF	4.785	4.631	0.285	1.356	1.566	0.325
Acetonitrile	4.682	4.519	0.296	1.625	1.789	0.333
DMSO	4.676	4.512	0.297	1.639	1.804	0.333

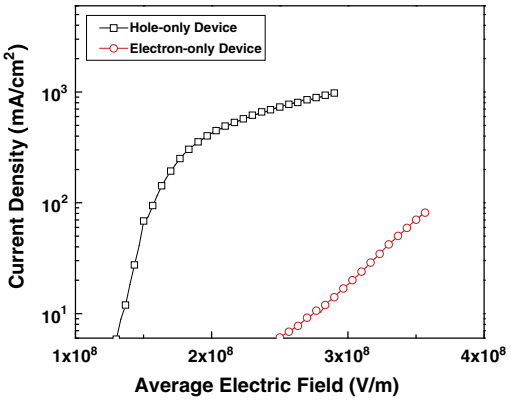

Fig. 5. The current characteristics as a function of the average electric field for hole-only and electron-only devices.

To further explore the application of **BDDAICZ** as the charge-transporting material in the OLEDs, two single carrier devices were prepared. First, a hole-only device, with the configuration of ITO/NPB (30 nm)/**BDDAICZ** (30 nm)/NPB (30 nm)/Al, was prepared to examine the hole-transporting capability of **BDDAICZ**. In which NPB (N,N′-bis-(1-naphthyl)-N,N′-diphenyl-1,10-biphenyl-4,4′-diamine) was used to block the electron from the cathode because the LUMO energy level of NPB is high enough to block electron injection. Then the other electron-only device, ITO/Alq_3 (30 nm)/**BDDAICZ** (30 nm)/Alq_3 (30 nm)/LiF (1 nm)/Al, was fabricated to examine the electron-transporting capability of this compound. In which Alq_3 (tris(8-quinolinolato)aluminum) as was used to block the hole from the anode because of its low HOMO level. Fig. 5 depicts the current-characteristics of the two devices as a function of the average electric field. As shown in Fig. 5, the hole-only device could conduct more significant currents than the electron-only device, indicating that **BDDAICZ** possesses the excellent hole-transporting property and it is a promising candidate as hole-transport material for OLEDs devices. The results of **BDDAICZ** as the charge-transporting material in the OLEDs are consistent with those of theoretical calculation. Further study on its application in OLEDs is being carried out in our laboratory.

Conclusion

In summary, a novel asymmetric compound, 2-benzothiazolyl-8-diphenylamino-5,11-dihexylindolo[3,2-b]carbazole **(BDDAICZ)**, was synthesized and characterized by elemental analysis, ^{1}H NMR, ^{13}C NMR and MS. **BDDAICZ** belongs to donor–π-donor–π-acceptor system comprising an indolo[3,2-b]carbazole moiety (as a skeleton and an electron donor), a diphenylamino moiety (as an electron donor) and a benzothiazole moiety (as an electron acceptor). The thermal, electrochemical, photophysical and

charge-transporting properties of **BDDAICZ** were characterized by the combination of experimental and theoretical methods. The results show that **BDDAICZ** has excellent thermal stability, electrochemical stability and hole-transporting properties, indicating its potential application as a hole-transporting material in OLEDs.

Acknowledgements

This work was supported by Natural Science Foundation of Shanxi Province (No. 2013011013-1), Scientific and Technological Innovation Programs of Higher Education Institutions in Shanxi Province (No. 2012005) and National Natural Scientific Foundation of China (No. 21376144) and Fund of Key Laboratory of Optoelectronic Materials Chemistry and Physics, Chinese Academy of Sciences (No. 2008DP173016). All the calculations have been performed with the advanced computing facilities of supercomputing centre of computer network information centre of Chinese Academy of Sciences. All the authors express their deep thanks.

Appendix A. Supplementary material

Supplementary data associated with this article can be found, in the online version, at http://dx.doi.org/10.1016/j.saa.2014.06.011.

References

[1] N.X. Hu, S. Xie, Z. Popovic, B.S. Ong, A.M. Hor, J. Am. Chem. Soc. 121 (1999) 5097–5098.
[2] Y.L. Wu, Y.N. Li, S. Gardner, B.S Ong, J. Am. Chem. Soc. 127 (2005) 614–618.
[3] Y.N. Li, Y.L. Wu, S. Gardner, B.S. Ong, Adv. Mater. 17 (2005) 849–853.
[4] Y.N. Li, Y.L. Wu, S. Gardner, B.S. Ong, Macromolecules 39 (2006) 6521–6527.
[5] H.P. Zhao, X.T. Tao, P. Wang, Y. Ren, J.X. Yang, Y.X. Yan, C.X. Yuan, H.J. Liu, D.C. Zou, M.H. Jiang, Org. Electron. 8 (2007) 673–682.
[6] H.P. Zhao, X.T. Tao, F.Z. Wang, Y. Ren, X.Q. Sun, J.X. Yang, Y.X. Yan, D.C. Zou, X. Zhao, M.H. Jiang, Chem. Phys. Lett. 439 (2007) 132–137.
[7] H.P. Zhao, F.Z. Wang, C.X. Yuan, X.T. Tao, J.L. Sun, D.C. Zou, M.H. Jiang, Org. Electron. 10 (2009) 925–931.
[8] P.T. Boudreault, S. Wakim, M.L. Tang, Y. Tao, Z. Bao, M. Leclerc, J. Mater. Chem. 19 (2009) 2921–2928.
[9] P.T. Boudreault, A.A. Virkar, Z. Bao, M. Leclerc, Org. Electron. 11 (2010) 1649–1659.
[10] M. Kirkus, J.V. Grazulevicius, S. Grigalevicius, R. Gub, W. Dehaen, V. Jankauskas, Eur. Polymer J. 45 (2009) 410–417.
[11] D. Velasco, V. Jankauskas, J. Stumbraite, J.V. Grazulevicius, V. Getautis, Synth. Met. 159 (2009) 654–658.
[12] S. Lengvinaite, J.V. Grazulevicius, S. Grigalevicius, R. Gub, W. Dehaen, V. Jankauskas, B. Zhang, Z. Xie, Dyes Pigm. 85 (2010) 183–188.
[13] M. Kirkus, J. Simokaitiene, J.V. Grazulevicius, V. Jankauskas, Synth. Met. 160 (2010) 750–755.
[14] J. Simokaitiene, E. Stanislovaityte, J.V. Grazulevicius, V. Jankauskas, R. Gu, W. Dehaen, Y.C. Hung, C.P. Hsu, J. Org. Chem. 77 (2012) 4924–4931.
[15] S.Y. Chen, J.B. Wei, K. Wang, C.G. Wang, D. Chen, Y. Liu, Y. Wang, J. Mater. Chem. C 1 (2013) 6594–6602.
[16] H.P. Shi, J.W. Yang, X.Q. Dong, Li Fang, C. Dong, M.M.F. Choi, Synth. Met. 179 (2013) 42–48.
[17] S.Y. Cai, G.J. Tian, X. Li, J.H. Su, H. Tian, J. Mater. Chem. A 1 (2013) 11295–11305.
[18] L.N. Yudina, J. Bergman, Tetrahedron 59 (2003) 1265–1275.
[19] P. Hohenberg, W. Kohn, Phys. Rev. 136 (1964) B864–B871.
[20] W. Kohn, L.J. Sham, Phys. Rev. 140 (1965) A1133–A1138.
[21] Andriy V. Kityk, J. Phys. Chem. A 116 (2012) 3048–3055.
[22] M. Mbarek, B. Zaidi, K. Alimi, Spectrochim. Acta, Part A: Mol. Biomol. Spectrosc. 88 (2012) 23–30.
[23] P. Gsiorski, K.S. Danel, M. Matusiewicz, T. Uchacz, W. Kuznikd, Ł. Pia, tek, A.V. Kityk, Mater. Chem. Phys. 132 (2012) 330–338.
[24] M.J. Frisch, G.W. Trucks, H.B. Schlegel, G.E. Scuseria, M.A. Robb, J.R. Cheeseman, G. Scalmani, V. Barone, B. Mennucci, G.A. Petersson, H. Nakatsuji, M. Caricato, X. Li, H.P. Hratchian, A.F. Izmaylov, J. Bloino, G. Zheng, J.L. Sonnenberg, M. Hada, M. Ehara, K. Toyota, R. Fukuda, J. Hasegawa, M. Ishida, T. Nakajima, Y. Honda, O. Kitao, H. Nakai, T. Vreven, J.A. Montgomery Jr., J.E. Peralta, F. Ogliaro, M. Bearpark, J.J. Heyd, E. Brothers, K.N. Kudin, V.N. Staroverov, R. Kobayashi, J. Normand, K. Raghavachari, A. Rendell, J.C. Burant, S.S. Iyengar, J. Tomasi, M. Cossi, N. Rega, J.M. Millam, M. Klene, J.E. Knox, J.B. Cross, V. Bakken, C. Adamo, J. Jaramillo, R. Gomperts, R.E. Stratmann, O. Yazyev, A.J. Austin, R. Cammi, C. Pomelli, J.W. Ochterski, R.L. Martin, K. Morokuma, V.G. Zakrzewski, G.A. Voth, P. Salvador, J.J. Dannenberg, S. Dapprich, A.D. Daniels, O. Farkas, J.B. Foresman, J.V. Ortiz, J. Cioslowski, D.J. Fox, Gaussian-09, Revision A.02, Gaussian Inc, Wallingford CT, 2009.
[25] J.Y. Jeon, T.J. Park, W.S. Jeon, J.J. Park, J. Jang, J.H. Kwon, J.Y. Lee, Chem. Lett. 36 (2007) 1156–1157.
[26] Z. Ge, T. Hayakawa, S. Ando, M. Ueda, T. Akiike, H. Miyamoto, T. Kajita, M. Kakimoto, Adv. Funct. Mater. 18 (2008) 584–590.
[27] T.M. Clarke, K.C. Gordon, W.M. Kwok, D.L. Phillips, D.L. Officer, J. Phys. Chem. A 110 (2006) 7696–7702.
[28] K.S. Danel, P. Gsiorski, M. Matusiewicz, S. Całus, T. Uchacz, A.V. Kityk, Spectrochim. Acta, Part A: Mol. Biomol. Spectrosc. 77 (2010) 16–23.
[29] E. Gondek, S. Całus, A. Danel, A.V. Kityk, Spectrochim. Acta, Part A: Mol. Biomol. Spectrosc. 69 (2008) 22–26.
[30] Y. Sun, X.H. Liang, Y.Y. Zhao, J. Fan, Spectrochim. Acta, Part A: Mol. Biomol. Spectrosc. 102 (2013) 194–199.
[31] L. Cisse, A. Djande, M. Capo-Chichi, F. Delatre, A. Saba, A. Tinea, J. Aaron, Spectrochim. Acta, Part A: Mol. Biomol. Spectrosc. 79 (2011) 428–436.
[32] J.N. Dmas, G.A. Crobys, J. Phys. Chem. 75 (1971) 991–1024.
[33] J.L. Brédas, R. Silbey, D.S. Boudreaux, R.R. Chance, J. Am. Chem. Soc. 105 (1983) 6555–6559.
[34] V. Promaraka, S. Ruchirawat, Tetrahedron 63 (2007) 1602–1609.
[35] R.A. Marcus, Rev. Mod. Phys. 65 (1993) 599–610.
[36] V. Coropceanu, J. Cornil, A. Demetrio, Y. Olivier, R. Silbey, J.L. Bredas, Chem. Rev. 107 (2007) 926–952.
[37] M.H. Tsai, H.W. Lin, H.C. Su, T.H. Ke, C.C. Wu, F.C. Fang, Y.L. Liao, K.T. Wong, C.I. Wu, Adv. Mater. 18 (2006) 1216–1220.
[38] L.Y. Zou, A.M. Ren, J.K. Feng, Y.L. Liu, X.Q. Ran, C.C. Sun, J. Phys. Chem. A 112 (2008) 12172–12178.